



A signature of 17 immune-related gene pairs predicts prognosis and immune status in HNSCC patients

Pan Jiang ^{a,*}, Yanli Li ^a, Zheng Xu ^a, Shengteng He ^{a,*}

^a Department of stomatology, Sanya Central Hospital, 146 the Fourth of Jiefang Road, 572000, Sanya, Hainan Province, China



ARTICLE INFO

Keywords:

HNSCC
Immune-related gene pairs
Prognosis signature
Immunotherapy
Bioinformatics

ABSTRACT

Head and neck squamous cell carcinoma (HNSCC) is an invasive malignancy with high worldwide mortality. Growing evidence has indicated a pivotal correlation between HNSCC prognosis and immune signature. This study investigated an immune-related gene pairs (IRGPs) signature to predict the prognostic value of HNSCC patients. We constructed IRGPs via integrating multiple IRG expression data sets. Moreover, we established the predictive model base on the IRGPs for HNSCC, and utilized multidimensional bioinformatics methods to validate the robustness of prognostic value of the IRGPs signature. In addition, we explored the relationship between the IRGPs model and immune status. Seventeen IRGPs signature was built as the predictive model which predicted prognosis independently and reliably for HNSCC. Compared to the high-risk group, the low-risk group demonstrated a distinctly favorable prognosis including overall survival (OS), disease-specific survival (DSS), and progression-free survival (PFS). The low-risk group showed higher-immune score and lower-tumor purity than the high-risk group. In addition, the low-risk group exhibited higher expression of Programmed cell death 1 ligand 1 (PD-L1) and Microsatellite instability (MSI) score, and lower expression of Tumor Immune Dysfunction and Exclusion (TIDE), which indicated the low-risk group was much more sensitive to immunotherapy. Lastly, the IRGs signature has achieved a higher accuracy than clinical properties for estimation of survival. The IRGPs model is an independent biomarker for estimating the prognosis, and could be also used to predict immunotherapeutic response in HNSCC patients. These findings may provide new ideas for novel biomarkers and may be helpful to formulate personalized immunotherapy strategy.

Introduction

Head and neck squamous cell carcinoma (HNSCC) is the sixth most common global cancer [1]. Nearly 50% patients die annually within the frame of 5-year survival rate, despite considerable advances in diagnosis and treatment in recent years [2,3]. Surgery is the first priority of therapeutic regimen, combined with chemotherapy and radiation therapy. Even though patients have the same clinical characteristics and pathological stages after similar treatments, they may have different prognosis and outcomes because of genetic heterogeneity [4]. Heterogeneous subsets of tumor with different molecular targets may lead to different resistance levels to cancer therapy and the progression of final clinical outcomes [5,6]. This is mainly due to the presence of heterogeneity of EGFR polymorphisms (variation) and clinical response, and EGFR variations has a better therapy outcome [7,8].

Growing evidence has manifested that the immune system plays a pivotal role during cancer initiation and progression [9,10]. Immunotherapy involves activation of anti-tumor immune responses to

cancer cells by selectively identifying and binding immunosuppressive proteins that are expressed on tumor cells, macrophages, regulatory T cells, and activation of T and B cells, thereby altering the tumor microenvironment [11,12]. A large number of antigens that can be used as potential targets for recognition by the immune system due to hundreds of coding exons mutations in some cancers. To date, many immune escape mechanisms have been identified [13,14], and despite the abundant expression of antigens, most cancers progress and escape immune system-mediated attack [13].

High-throughput gene expression assays can improve our understanding of cancer biology and identify predictive features in depth analysis, but in terms of the number of reliable reports of gene expression data, the biology and prediction of HNSCC is very limited. We aim to provide new biomarkers that can effectively predict the prognosis of HNSCC patients and monitor the tumor immune microenvironment. In our study, immune genes that were significantly associated with prognosis were screened. Based on these genes, a personalized prognostic

* Corresponding authors.

E-mail addresses: jiangpanprivate@163.com (P. Jiang), heshengteng1972@163.com (S. He).

signature was established and validated via integrating immune-related gene pairs (IRGPs) of HNSCC.

Materials and methods

Data acquisition

Our study used public data to conduct a comprehensive analysis based on The Cancer Genome Atlas Program (TCGA) and Gene Expression Omnibus (GEO). From these databases, we download the clinical and RNA-seq expression data of HNSC patients. We obtained data of 528 HNSCC patients from TCGA website as training dataset, including carcinomas of 18 alveolar ridge, 27 base of tongue, 23 buccal mucosa, 63 floor of mouth, 7 hard palate, 10 hypopharynx, 117 hypopharynx, 3 lip, 73 oral cavity, 133 oral tongue, 9 oropharynx, and 45 tonsil, and 97 patients of gene expression data and its corresponding clinical data with HNSCCs from GSE41613 as the validation dataset, defined as cancers of the alveolar ridge, buccal mucosa, floor of mouth, hard palate, oral cavity, oral tongue, and oropharynx. The Immunology Database and Analysis Portal (Immport), one of the largest open repositories, is a platform that it provides human immunological data [15]. From this website, we acquired 2498 immune related genes (IRGs) for further immunity analysis.

Construction of a predictive-related Immune related gene pairs (IRGPs)

To obtain a score for each IRGP, a pairwise comparison between the expression values of immune-related genes was performed in each sample. If the expression level of the first IRG is higher than the following one in a particular IRGP, the IRGP score is 1; otherwise, the score is 0. To avoid biases and unrepeatability, some IRGPs were removed because they had a unique value of 0 or 1 in more than 80% of the samples in the study dataset, and the remaining as initial candidate IRGPs. Next, we performed a univariate Cox regression analysis ($p < 0.0001$) to obtain the significant prognostic-related IRGPs with HNSCC. In addition, we performed the least absolute shrink age and selection operator (LASSO) Cox regression (iteration = 1000) using glmnet R package to acquire a well-balanced prognostic model after primary filtration, and 17 IRGPs were ultimately selected as our prognostic model. To classify patients into low-risk and high-risk groups, the time-dependent receiver operating characteristic (ROC) curve analysis was used to determine the optimal cut-off score of IRGPs at 1 year for overall survival (OS).

Validation of the IRGPs signature

To predict the reliability and stability of prognostic model based on the IRGPs, we compared the overall survival between high and low risk groups in TCGA and GSE41613 cohort with HNSCC, using R (survival package) to obtain the Kaplan-Meier curve. Moreover, we performed univariate and multivariate cox proportional-hazards analyses to evaluate our prognostic model with other clinical characteristics to validate our model to be an independent prognostic factor.

Assessment of immune-microenvironment

Estimation of STromal and Immune cells in MAlignant Tumor tissues using Expression data (ESTIMATE) is a tool to predict the fraction of stromal and immune cells in tumor samples utilizing gene expression signatures [16]. Immune score and tumor purity were assessed based on the ESTIMATE algorithm to TCGA gene expression data [17].

Estimation of immune cells infiltration

Cell type identification by estimating relative subset of known RNA transcripts (CIBERSORT), an approach to infer immune cells in tumor

transcriptome, was utilized to quantify the proportion of 22 immune cells from microarray data in HNSCC samples. We performed the CIBERSORT algorithm to analyze the normalized gene expression data, running with 1,000 permutations [18,19]. CIBERSORT p-value reflects the result significance between low- and high- risk groups, and the threshold was identified if the $p < 0.05$.

Immunotherapeutic response prediction

The immune checkpoint pathways are associated with tumor immune escape. Therefore, immune checkpoint inhibitors can enhance anti-cancer immunity [20,21]. As mentioned before, we employed Tumor Immune Dysfunction and Exclusion (TIDE) algorithm to predict the clinical response of immune checkpoint inhibitors [19,22]. Microsatellite instability [23] (MSI) is a form of hypermutation caused by defects in the mismatch repair mechanism. Through MSI algorithm, we evaluated the relationship with immune response and prognosis.

Gene set enrichment analysis (GSEA)

We utilized fgsea R package to perform gene set enrichment analysis to compare the differential enrichment of gene sets between the high and low risk groups. We downloaded GO gene sets in GSEA database for this study. The thresholds of analyses with p -value < 0.05 , indicating functional annotations enriched significantly.

Independence of the IRGPs-based model from other HNSC patients' clinical characteristics

We performed univariate and multivariate Cox regression analyses to examine whether the prognostic model was independent variable, considering other conventional clinical features (age, gender, grade, tumor/node/metastasis (TNM) stage) in HNSCC patients.

Construction of a Nomogram Model for prognostic risk prediction

We established a nomogram using multivariate Cox regression of clinical features to visualize the prognostic value of different risk scores. The analysis was applied through the rms R package to integrate the IRGPs signature and clinical/pathologic features.

Results

Construction of IRGPs signature in the training dataset

Our study included a total of 528 HNSCC patients. We downloaded 2,498 IRGs from the ImmPort database, and 419 IRGs were measured in the TCGA and GEO cohort. Then 7,396 IRGPs were constructed as described previously. The study design was displayed in Supplemental Fig. 1. We subsequently explored the correlation between the IRGPs and prognosis employing univariate Cox regression analysis in HNSCC patients with overall survival. Then, LASSO-penalized Cox analysis was conducted to narrow the number of IRGPs to 17 over 1000 repetitions in the final model. To divide all the samples into the high- or low-immune risk groups, we calculated the risk score of each sample, then we performed ROC curve analysis at 1 year in the training group for OS and set the optimal cut off at - 0.014 (Fig. 1A). Patients with higher risk score than - 0.014 will be counted in high risk group, otherwise, that be counted in low risk group (Fig. 1B-C). The survival overview was showed in Fig. 1D. Kaplan-Meier analysis showed high-risk groups had significantly worse OS than low-risk ($p < 0.001$; Fig. 1E). We further explored its prognostic value based on disease-specific survival (DSS), and progression-free survival (PFS). High-risk HNSCC patients were also inclined to have worse DSS ($p < 0.001$; Fig. 1F), and PFS ($p < 0.001$; Fig. 1G). To further evaluate the prognostic reliably of the IRGPs for other clinical factors in the train cohort, HNSCC patients were

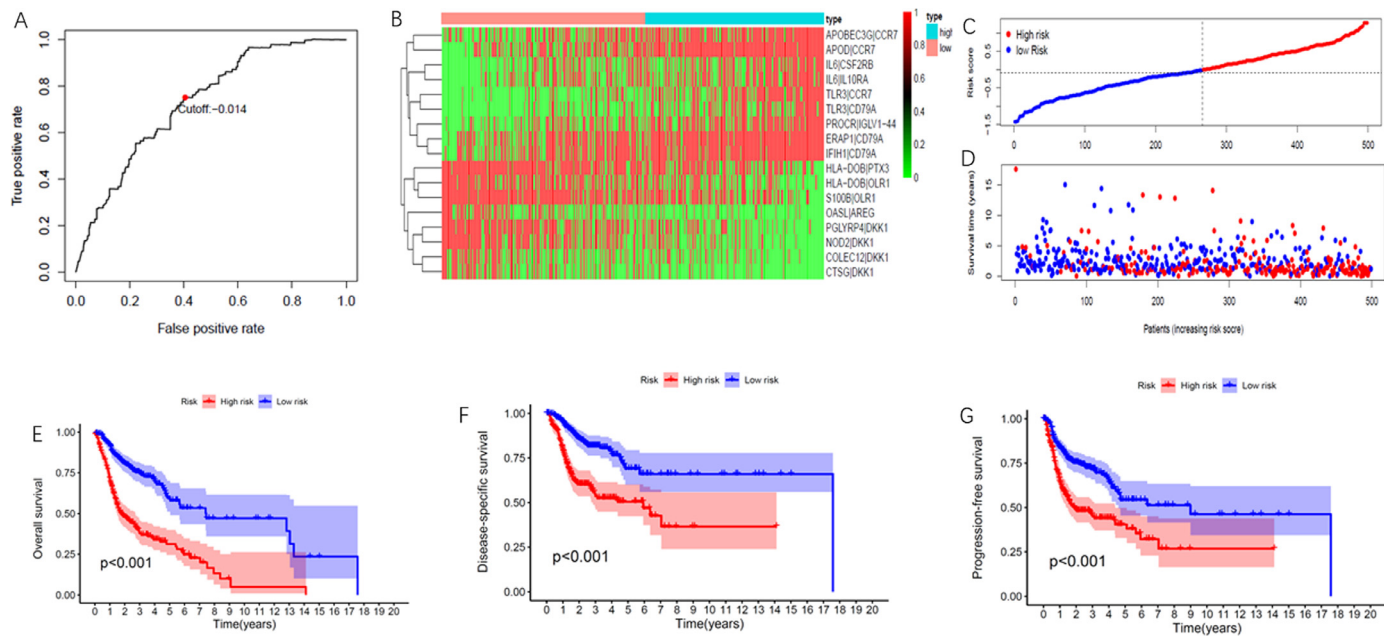


Fig. 1. Construction of IRGPs model for HNSCC patients.

(A) Time-dependent ROC curve for IRGPs in the TCGA dataset. The optimal cut off of -0.014 was used to divide patients into low- or high-risk groups. (B) Heatmap of 17 IRGPs profiles in the high- and low-risk groups. (C) The distribution of the IRGPs-based risk score. (D) Vital statuses of patients in the high- and low-risk groups. (E–G) Kaplan-Meier survival curves of the relative OS, DSS, and PFS between the high- and low-risk groups.

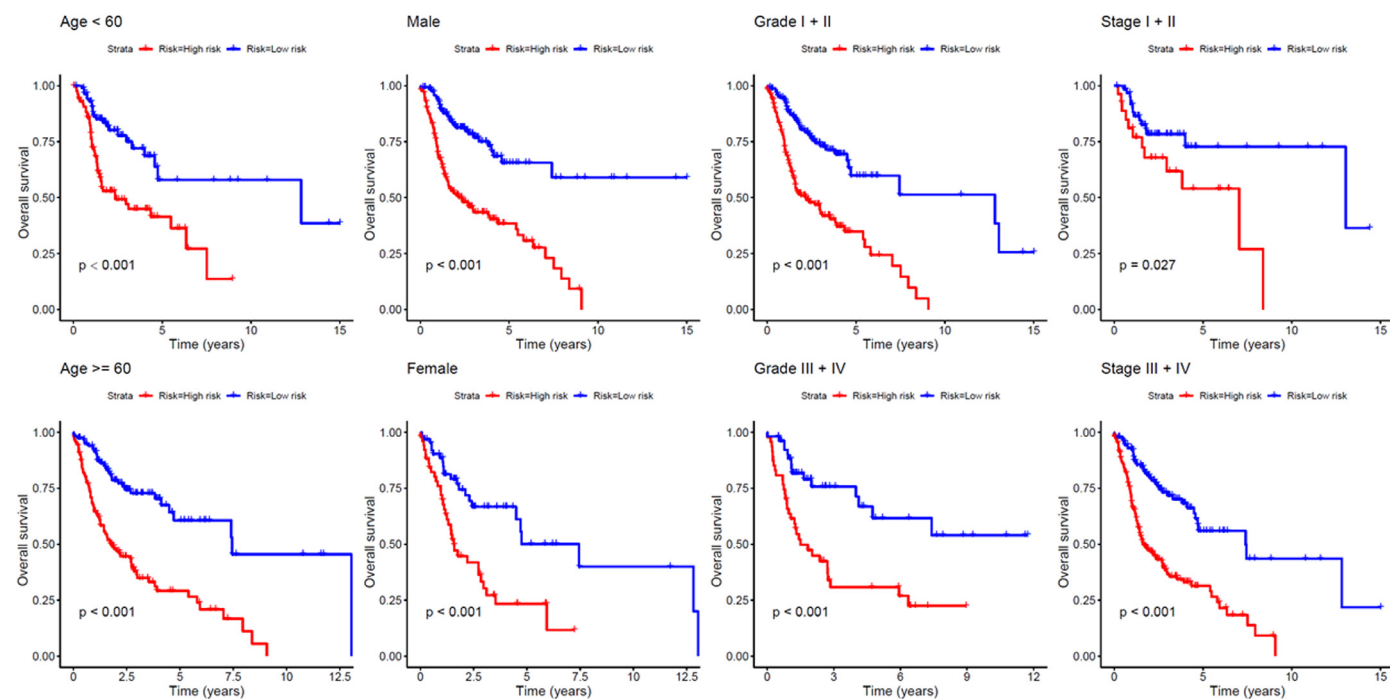


Fig. 2. Kaplan-Meier analysis of OS for HNSCC patients.

Patients were classified according to age (age < 60 and age ≥ 60), gender (male and female), grade (grade I+II and grade III+IV), and stage (stage I+II and stage III+IV).

stratified into different subgroups on the basis of clinical characteristics, including age (age < 60 and age ≥ 60), gender (male and female), grade (grade I+II and grade III+IV), stage (stage I+II and stage III+IV). Kaplan-Meier overall survival curves also showed that high-risk groups had considerably poorer OS of different subgroups than low-risk patients (Fig. 2), which further indicated the prediction of IRGPs model is excellent.

Validation of IRGPs model in the validation dataset

To predict the ability of prognostic model, we validated the reliability and stability using survival data of GSE41613 dataset based on the IRGPs. The risk scores of HNSCC patients were calculated using the calculated score mentioned in methods, and then patients with HNSCC were classified into low- and high-risk groups (Fig. 3A-3C). Compared to

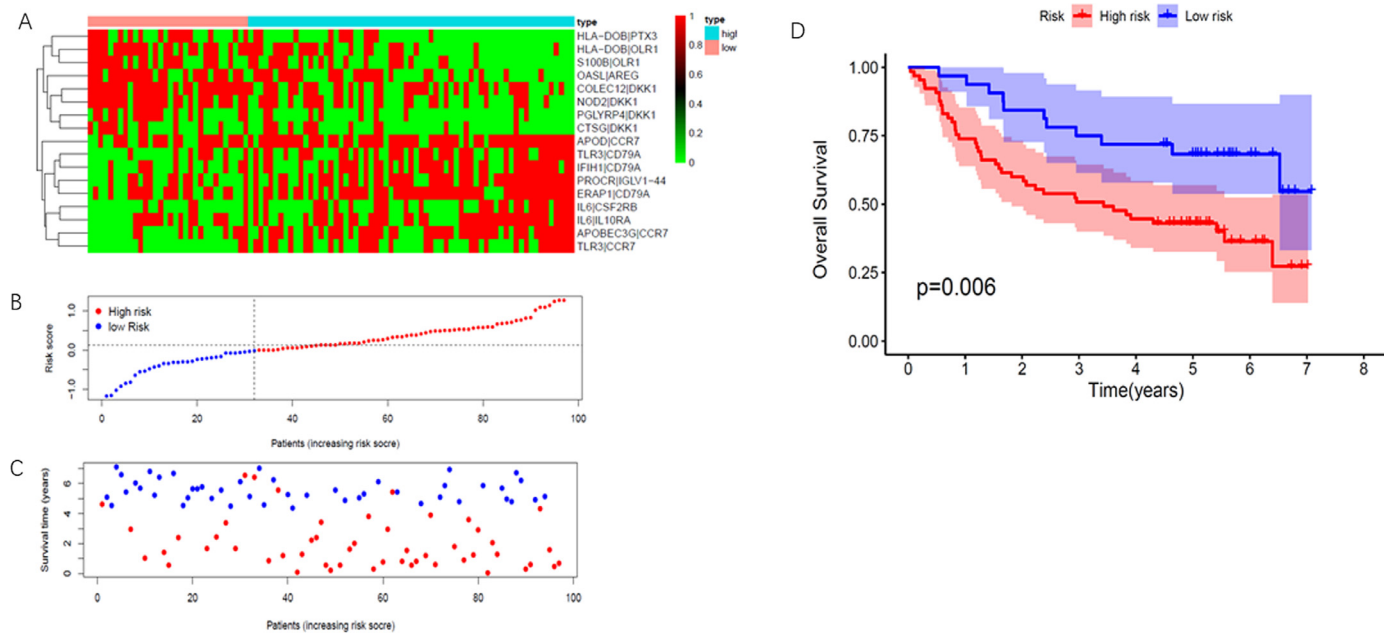


Fig. 3. Validation of the IRGPs model for HNSCC patients using GEO database.

(A) Heatmap of 17 IRGPs profiles in the high- and low-risk groups. (B) The distribution of the IRGPs-based risk score. (C) Vital statuses of patients in the high- and low-risk groups. (D) Kaplan-Meier curves OS between high- and low-risk groups.

the low risk group, the high-risk patients in the validation dataset had a markedly poorer OS ($p = 0.006$; Fig. 3D), the finding of overall survival difference in high/low-risk group was consistent with the training group.

Assessment of immune regulatory markers between high- and low-risk groups

Differences in immune infiltration were then explored to distinguish high- and low-risk HNSCC patients. Based on the ESTIMATE algorithm, the immune score in the low-risk group were higher than those in the high-risk group (Fig. 4A). Moreover, we compared the tumor purity of the two HNSCC subtypes, and obtained opposite trends: high-risk group ranked higher (Fig. 4B). As a hopeful strategy to treat many cancers, Immune checkpoint inhibitor has been emerged in recent years. We subsequently investigated the expression of pivotal immunomodulator with PD-L1. Low-risk patients with HNSC had higher expression of immune checkpoint molecules than high-risk patients (Fig. 4C). Then, we harnessed the TIDE algorithm to predict the likelihood of response to immunotherapy. Interestingly, we found that low-risk group was more likely effective for immunotherapy than high-risk group (Fig. 4D). As showed in Fig. 4E, The MSI score of the low-risk group was significantly lower than that of the high-risk group. These data further supported our analysis that low-risk subtype had better prognosis, and might be a more promising treatment for responding to immunotherapy.

Through the CIBERSORT, we evaluated the differences in the 22 immune infiltration cells between two groups in HNSCC samples, the contents of 16 immune cells were different between the two groups (5A). As illustrated in Fig. 5B, the infiltration of nine immune cells were significantly different between the two groups ($p < 0.001$), the infiltration level of Plasma cells, B cells naive, T cells CD8, T cells follicular helper and T cells regulatory (Tregs) were higher in the low-risk group, and the contents of T cells CD4 memory resting, Macrophages M0, Macrophages M2 and NK cells resting were higher in the high-risk group.

Gene set enrichment analysis (GSEA)

We assigned the TCGA training cohort into low risk group and high risk group, then GSEA was carried out to explore the signaling pathways

that were significantly altered. The results illustrated that four pathways were identified (Fig. 6) including “IMMUNE RESPONSE REGULATING CELL SURFACE RECEPTOR SIGNALING PATHWAY”, “REGULATION OF LYMPHOCYTE ACTIVATION”, “REGULATION OF IMMUNE EFFECTOR PROCESS”, and “SENSORY PERCEPTION OF SMELL”, which indicated that these signaling pathways played a crucial role in HNSCC progression.

Association between IRGPs model and clinicopathological factors

Considering other conventional clinical properties in the TCGA dataset, we performed univariate and multivariate Cox regression analysis to elucidate whether the prognostic model for OS is an independent indicator. Univariate Cox regression analysis revealed that age, pathologic stage, and risk score were correlated with poorer survival ($p < 0.001$; Fig. 7A), and multivariate Cox regression analysis revealed that the risk score may be considered as a specific prognostic indicator for HNSCC ($p < 0.001$; Fig. 7B). The AUC value for the IRGPs model of risk score in TCGA dataset was 0.736 (Fig. 7C). In GEO dataset, univariate and Cox regression analyses also showed the similar results that the risk score served as an independent factor for predicting the OS of HNSCC patients (Fig. 7D-E), and the AUC value for the IRGPs model of risk score was 0.695 (Fig. 7F). To further elucidate whether the prognostic models for DSS and PFI were independent for other clinical properties in TCGA, we carried out univariate and multivariate Cox regression analyses. Then we found that these models were also considerable in Cox regression analyses ($p < 0.001$; Supplemental Fig. 2-3). Thus, these results suggested that the IRGPs model could predict independently for specific clinical factors in HNSCC patients.

Construction and validation of a predictive nomogram

To provide a quantitative method for clinicians to predict the survival probability of HNSCC patients, we constructed a nomogram to predict the probability of the 1-, 2- and 3-year OS in the TCGA cohort (Fig. 8A). The factors of nomogram included age, pathologic stage, gender, grade, risk score. The C-index of the IRGPs model for evaluation of 1-, 2-, and 3-year OS displayed superior predictive performance than that of other clinical properties (Fig. 8B). Moreover, the calibration plots

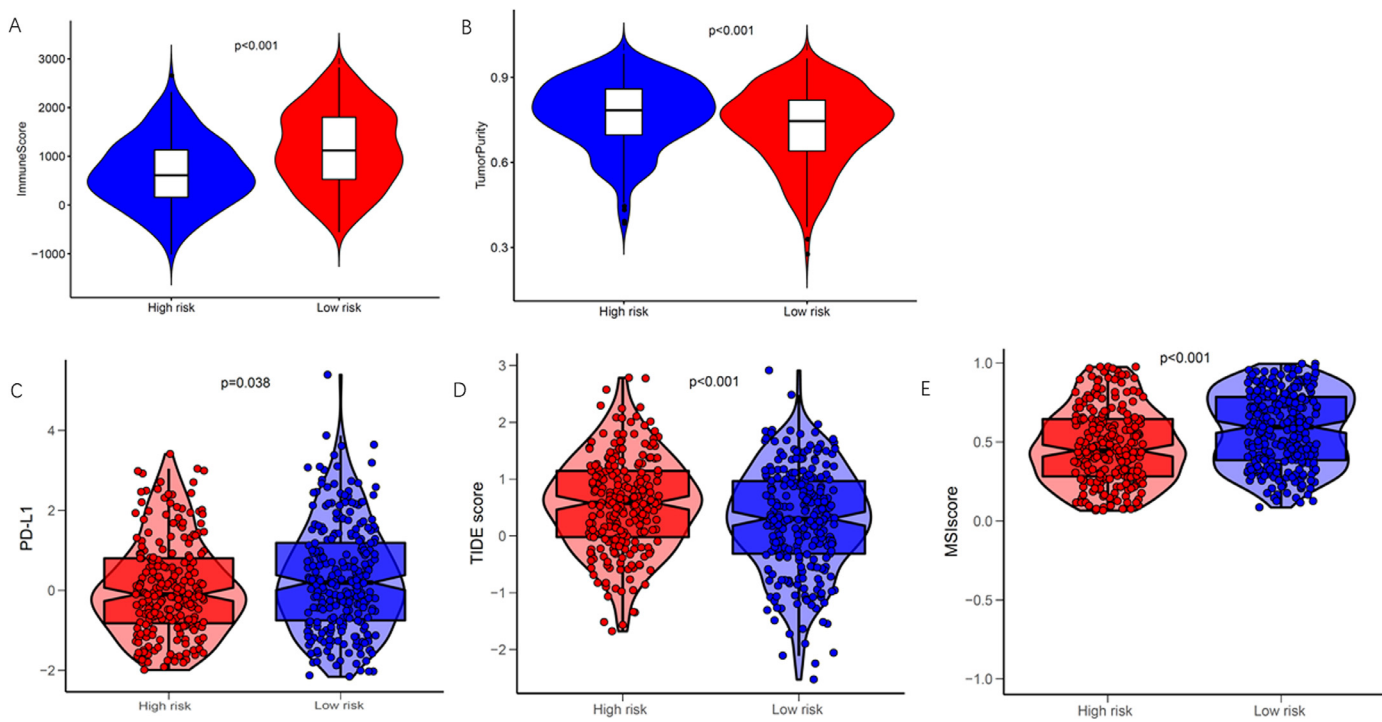


Fig. 4. Tumor immune microenvironment between high- and low-risk groups with HNSCC patients.

(A) Immune scores and (B) Tumor purity between high- and low-risk patients. (C) PD-L1 expressed between high- and low-risk patients. (D) TIDE and (E) MSI prediction score between high- and low-risk patients.

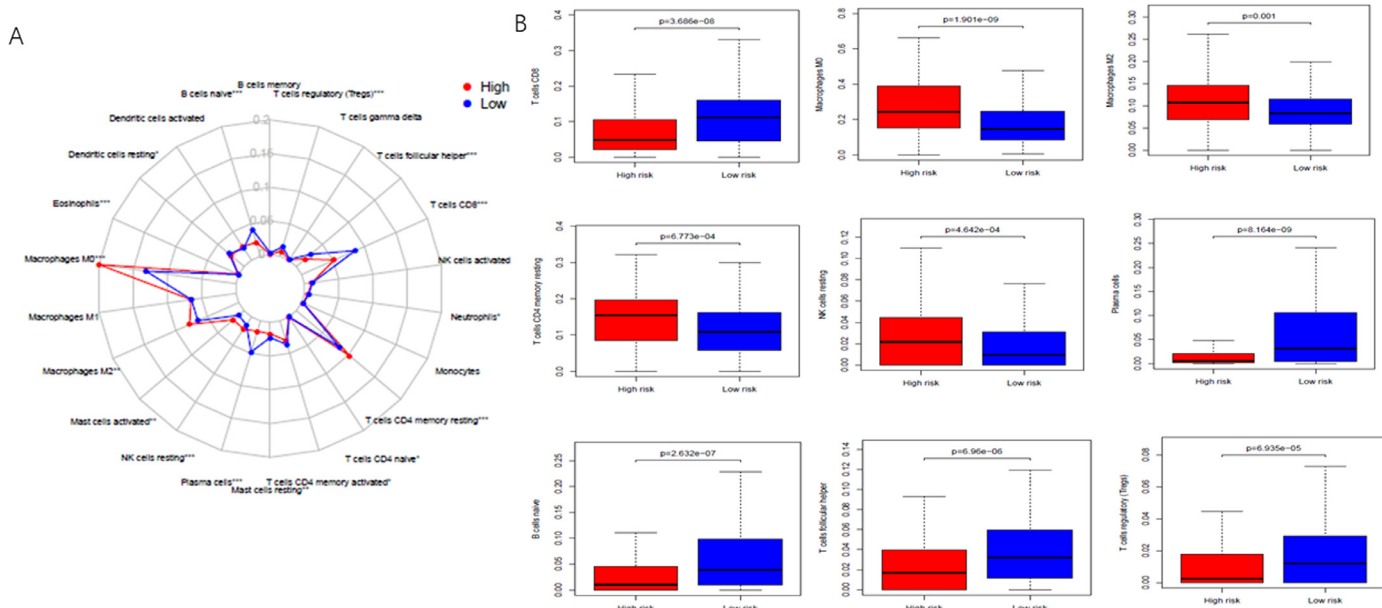


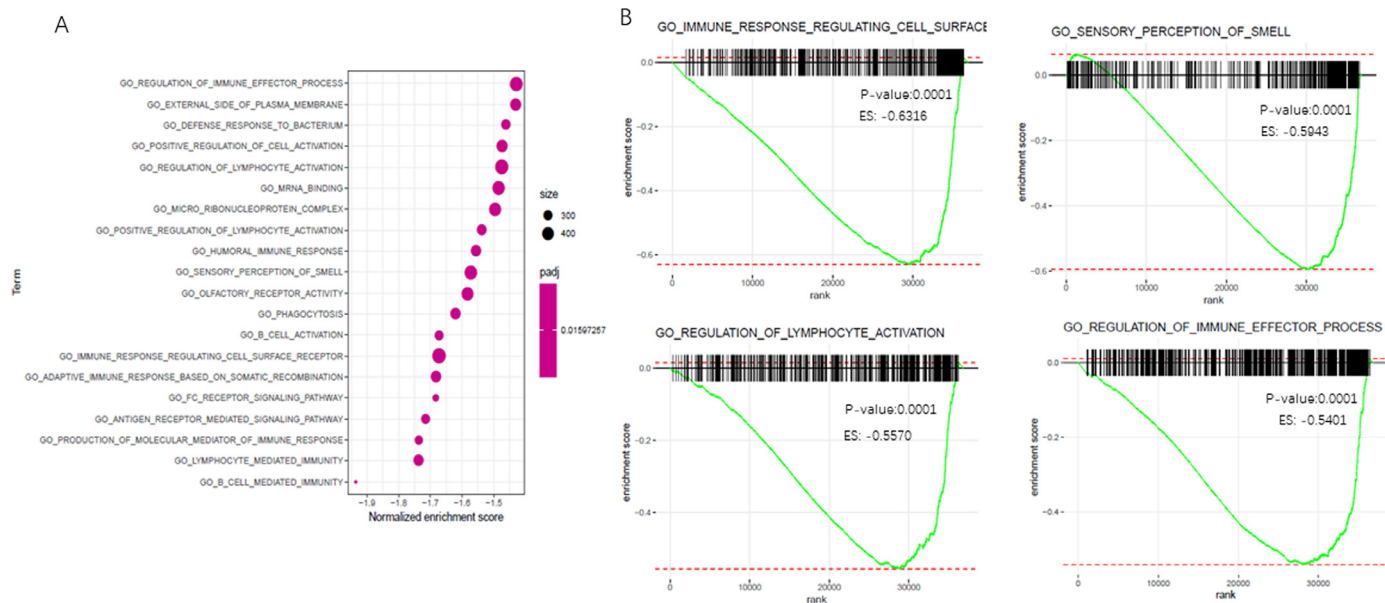
Fig. 5. Immune infiltration status in IRGPs risk groups.

(A) Summary of the 22 immune cells abundance estimated for different subtypes. (B) The abundance distribution of nine immune cells with significant differences in different risk groups.

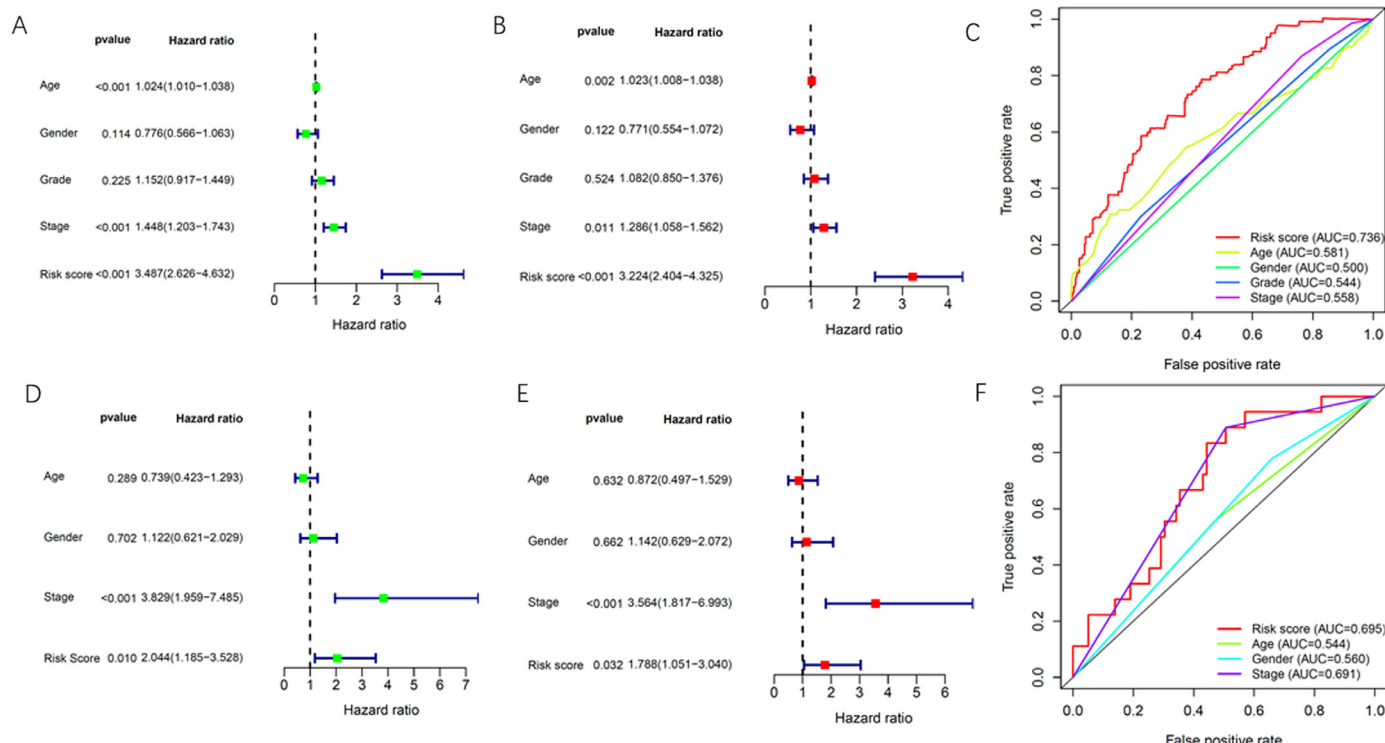
of the nomogram showed that the bias-corrected line was close to the ideal curve (the 45-degree line), which displayed superior agreement between the predicted 1-, 2-, and 3-year OS rates and actual observations (Fig. 8C). In total, these results indicated that our IRGPs model had favorable efficacy for predicting both short or long term OS for HNSCC patients than conventional clinical characteristics.

Discussion

Most HNSCC patients have a poor prognosis because of advanced cancer when diagnosed, despite considerable advancements in diagnosis and treatment in recent years [2,24]. With intensive studies in the immune molecular mechanisms, precision oncology has become reality

**Fig. 6.** Functional enrichment of 17 IRGPs.

(A) Top 20 most significant Gene Ontology (GO) terms identified by GO analysis. (B) gene set enrichment analysis (GSEA).

**Fig. 7.** Correlations between the IRGPs model and clinical factors with OS based on TCGA and GEO databases.

Univariate and multivariate Cox analyses of clinical factors and the IRGPs model based on (A-B) TCGA and (D-E) GEO databases. Comparison of time-dependent ROC curves among the age, gender, grade, stage, and IRGPs-model based on (C) TCGA and (F) GEO databases.

for several types of cancers [25,26]. However, the current markers have certain limitations in predicting HNSC prognosis [27]. Therefore, it is urgent to determine effective therapeutic regimens and novel prognostic signatures. Gene expression profile standardization is tough due to inherent biological heterogeneity of caners and technical bias, previous predictive risk models still have obstacles to transform into

clinical practice. Compared with the traditional prognostic model, the pairwise comparison and score calculation of each IRGP were based on the gene expression entirely from the same sample. Although from different sequencing platforms, our IRGP signature does not require gene expression profiles preprocessing. Previous researches have proved the effectiveness of this method [28].

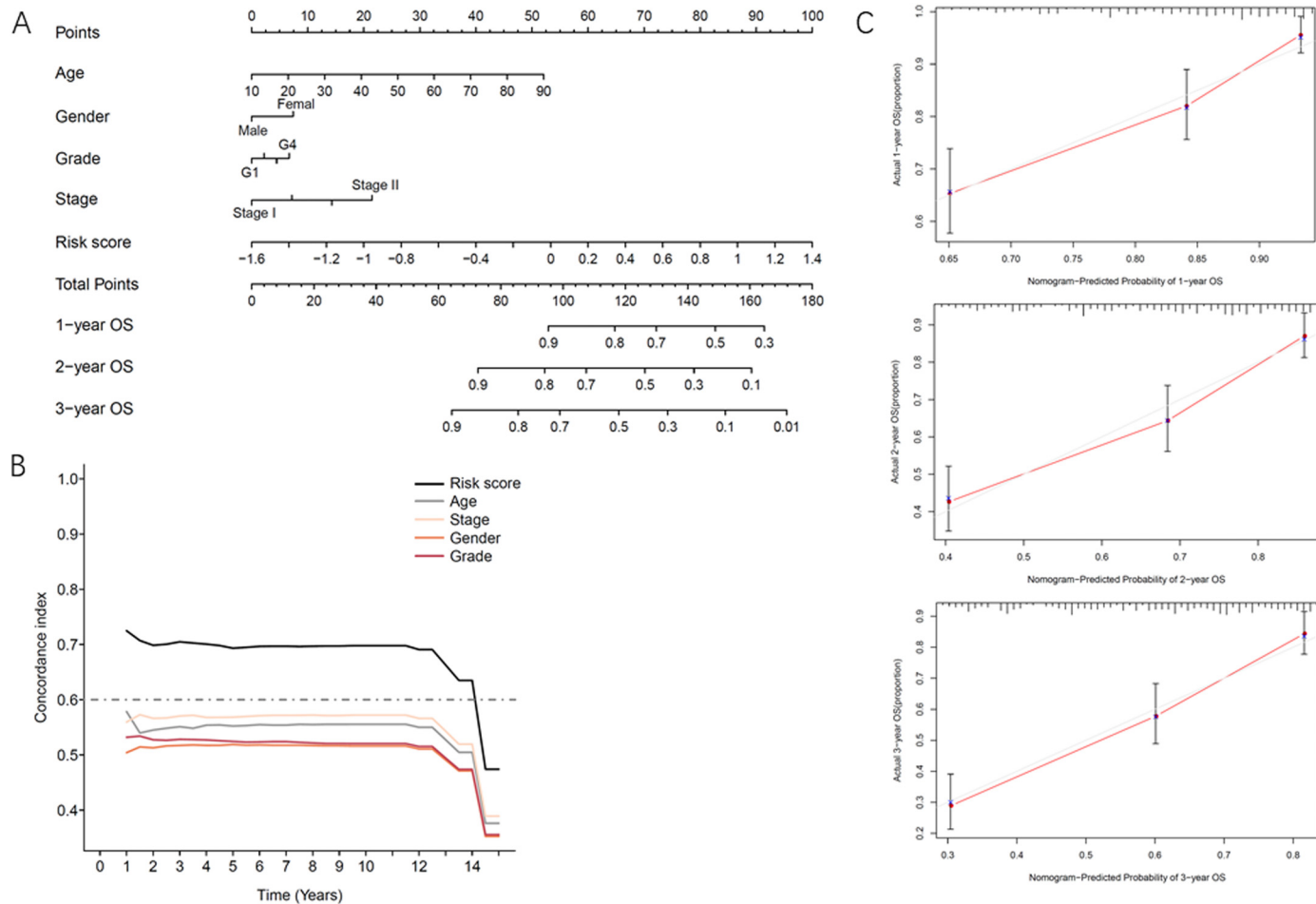


Fig. 8. Nomogram for predicting the probability of 1-, 2-, and 3-year OS for HNSCC patients in the TCGA database.

(A) Nomogram for predicting the probability of 1-, 2-, and 3-year OS for patients with HNSCC. (B) The C-index based on the nomogram for evaluating the probability of OS. (C) Calibration plot of the nomogram for predicting OS at 1, 2, and 3 years.

In the present study, we identified the IRGPs signature which contains 17 IRGPs consisting of 24 unique IRGs to predict survival for HNSCC patients, including OS, DSS, and PFS based on TCGA database, and we got the similar results in the GEO database that the low-risk group had better oncological outcomes than the high-risk group. In addition, we constructed risk model for comparative analysis by combining 17 IRGPs signature with the clinical/pathologic characteristics, HNSCC patients were stratified into subgroups to further validate the independent predictive value of the IRGPs signature. As a result, there are significant differences in the overall survival rate of each two subtypes. The stratification analysis indicated that the IRGPs model could effectively predict the overall survival regardless of the clinical properties.

Cancer microenvironment and immune cell infiltration are reported to be correlated with cancer prognosis [29]. The prognostic markers related to the tumor immune microenvironment may open up new prospects for the development of new predictive biomarkers and improving immunotherapy with HNSCC patients. Previous literatures demonstrated B cells naive was an anti-cancer immune cell [30]. In addition, macrophagem2 [31,32] had been shown to be related with poor prognosis while T cells CD8 [33] indicated better prognosis in a variety of cancer types. Increased B/plasma cell and T cell infiltration was associated with good prognosis [34]. Immunoactivation of B cells, dendritic cells, T cells, and natural cells contributed to tumor suppression [35]. Natural killer (NK) cells are important effectors in the first line of defense. In the tumor microenvironment, TGF β , IL-6 and IL-10 inhibit the activity of NK cells to attenuate the antitumor response of NK cells

and promote tumor evasion through affecting immunosuppressive cells and antagonizing the effect of stimulatory cytokines [36]. These results are consistent with our study. In view of current findings, immune cell might play a role in the prognostic differences observed between risk groups as defined by immune characteristics.

Programmed cell death 1 (PD-1) is an immune checkpoint receptor that expressed on activated T and B cells and binds to programmed cell death 1 ligand 1 (PD-L1) [37], and then inhibiting the activation and proliferation of T cells. Tumor cells can avoid immune attack more effectively within the tumor microenvironment [38,39]. Antibodies against PD-1 are effective in treating a variety of cancers and improve OS [40,41]. According to Luchini et al. [42] reported, MSI and PD-1/PD-L1 expression were significant factors of immune checkpoint blockade therapy. There is evidence indicated that increasing MSI positively correlated with high survival rate [43]. TIDE prediction showed that the low-risk group was more promising treatment for responding to immunotherapy. Based on the above evidence, we speculate that the predictive model based on IRGPs may act as reliable immune-related biomarker for cancer therapy.

Next, we combined the 17 IRGPs with the clinical traits of HNSCC patients from TCGA database and programmed risk modules for cox regression analysis. The results revealed that IRGPs model predicted HNSCC prognosis independently with the traditional clinical risk factors. ROC analysis indicated that it was superior to conventional clinical features in predicting HNSCC patients. Similarly, cox proportional-hazards analysis revealed that the independence of predictive performance of the

17 IRGPs relative to conventional clinicopathological properties both in training data set and validation data set. Survival analysis and univariate/multivariate cox regression analysis have not only proved the prognostic value of IRGPs signatures, but also proved to be an independent prognostic factor. Furthermore, the results of GSEA results showed that it was evident enrichments in immune regulation and lymphocyte activation regulation signaling pathways.

In conclusion, our IRGPs signature is robust biomarker for the prognosis of HNSCC through reliable evidence. The IRGPs model is an independent biomarker for estimating the prognosis in HNSCC patients, and may be helpful to formulate personalized immunotherapy strategy.

Author contributions statement

Pan Jiang participated in the design of the study and drafted the manuscript. Zheng Xu carried out the data collection and data interpretation. Yanli Li carried out the data analysis and statistical analysis. Shengteng He participated in the design of the study and revised the manuscript. All authors read and approved the final manuscript.

Declaration of Competing Interest

The authors declare that they have no known competing financial interests or personal relationships that could have appeared to influence the work reported in this paper.

Acknowledgments

The study was supported by Sanya Medical And Health Science And Technology innovation project (2018YW05). No benefits in any form have been or will be received from a commercial party directly or indirectly related to the subject of this article.

Supplementary materials

Supplementary material associated with this article can be found, in the online version, at doi:10.1016/j.tranon.2020.100924.

References

- [1] N. Vigneswaran, M.D. Williams, Epidemiologic trends in head and neck cancer and aids in diagnosis, *Oral Maxillofac. Surg. Clin. N. Am.* 26 (2014) 123–141.
- [2] S. Ausoni, P. Boscolo-Rizzo, B. Singh, M.C. Da Mosto, G. Spinato, G. Tirelli, R. Spinato, G. Azzarello, Targeting cellular and molecular drivers of head and neck squamous cell carcinoma: current options and emerging perspectives, *Cancer Metab. Rev.* 35 (2016) 413–426.
- [3] K. Lee, J.W. Chang, C. Oh, L. Liu, S.N. Jung, H.R. Won, Y.I. Kim, K.S. Rha, B.S. Koo, HOXB5 acts as an oncogenic driver in head and neck squamous cell carcinoma via EGFR/Akt/Wnt/β-catenin signaling axis, *Eur. J. Surg. Oncol.* (2019).
- [4] W. Chang, X. Gao, Y. Han, Y. Du, Q. Liu, L. Wang, X. Tan, Q. Zhang, Y. Liu, Y. Zhu, Y. Yu, X. Fan, H. Zhang, W. Zhou, J. Wang, C. Fu, G. Cao, Gene expression profiling-derived immunohistochemistry signature with high prognostic value in colorectal carcinoma, *Gut* 63 (2014) 1457–1467.
- [5] M. Kleppé, R.L. Levine, Tumor heterogeneity confounds and illuminates: assessing the implications, *Nat. Med.* 20 (2014) 342–344.
- [6] N. McGranahan, C. Swanton, Clonal Heterogeneity, Tumor Evolution, Past, present, and the future, *Cell* 168 (2017) 613–628.
- [7] V. Jurisic, V. Vukovic, EGFR polymorphism and survival of NSCLC patients treated with TKIs, *A Syst. Rev. Meta-Anal.* (2020) 1973241.
- [8] V. Jurišić, J. Obradović, S. Pavlović, N. Djordjević, Epidermal growth factor receptor gene in non-small-cell lung cancer: the importance of promoter polymorphism investigation., *Anal. Cell Pathol. (Amsterdam)* (2018) 6192187.
- [9] H. Angell, J. Galon, From the immune contexture to the Immunoscore: the role of prognostic and predictive immune markers in cancer, *Curr. Opin. Immunol.* 25 (2013) 261–267.
- [10] A.J. Gentles, A.M. Newman, C.L. Liu, S.V. Bratman, W. Feng, D. Kim, V.S. Nair, Y. Xu, A. Khuong, C.D. Hoang, M. Diehn, R.B. West, S.K. Plevritis, A.A. Alizadeh, The prognostic landscape of genes and infiltrating immune cells across human cancers, *Nat. Med.* 21 (2015) 938–945.
- [11] J. Gong, A. Chehrazi-Raffle, S. Reddi, R. Salgia, Development of PD-1 and PD-L1 inhibitors as a form of cancer immunotherapy: a comprehensive review of registration trials and future considerations, *6* (2018) 8.
- [12] S. Kruger, M. Ilmer, S. Kobold, B.L. Cadilha, S. Endres, S. Ormanns, G. Schuebbe, B.W. Renz, J.G. D'Haese, H. Schloesser, V. Heinemann, M. Subklewe, S. Boeck, J. Werner, M. von Bergwelt-Baildon, Advances in cancer immunotherapy 2019 - latest trends, *J. Exp. Clin. Cancer Res.* 38 (2019) 268.
- [13] T.F. Gajewski, H. Schreiber, Y.X. Fu, Innate and adaptive immune cells in the tumor microenvironment, *Nat. Immunol.* 14 (2013) 1014–1022.
- [14] T.R. Medler, T. Cotechini, L.M. Coussens, Immune response to cancer therapy: mounting an effective antitumor response and mechanisms of resistance, *Trends Cancer* 1 (2015) 66–75.
- [15] S.A.-O. Bhattacharya, P.A.-O. Dunn, C.G. Thomas, B. Smith, H. Schaefer, J. Chen, Z. Hu, K.A. Zalocusky, R.D. Shankar, S.S. Shen-Orr, E.A.-O. Thomson, J. Wiser, A.A.-O. Butte, ImmPort, toward repurposing of open access immunological assay data for translational and clinical research.
- [16] K. Yoshihara, M. Shahmoradgoli, E. Martínez, R. Vegesna, H. Kim, W. Torres-Garcia, V. Treviño, H. Shen, P.W. Laird, D.A. Levine, S.L. Carter, G. Getz, K. Stemke-Hale, G.B. Mills, R.G. Verhaak, Inferring tumour purity and stromal and immune cell admixture from expression data, *Nat. Commun.* 4 (2013) 2612.
- [17] K. Daily, S.J. Ho Sui, L.M. Schriml, P.J. Dexheimer, N. Salomon, R. Schroll, S. Bush, M. Keddache, C. Mayhew, S. Lotia, T.M. Perumal, K. Dang, L. Pantano, A.R. Pico, E. Grassman, D. Nordling, W. Hide, A.K. Hatzopoulos, P. Malik, J.A. Cancelas, C. Lutzko, B.J. Aronow, L. Omberg, Molecular, phenotypic, and sample-associated data to describe pluripotent stem cell lines and derivatives, *Sci. Data* 4 (2017) 170030.
- [18] R. Zhou, J. Zhang, D. Zeng, H. Sun, X. Rong, M. Shi, J. Bin, Y. Liao, W. Liao, Immune cell infiltration as a biomarker for the diagnosis and prognosis of stage I-III colon cancer, *Cancer Immunol. Immunother.: CII* (2018).
- [19] F. Xu, H. Zhang, J. Chen, L. Lin, Y. Chen, Immune signature of T follicular helper cells predicts clinical prognostic and therapeutic impact in lung squamous cell carcinoma, *Int. Immunopharmacol.* 81 (2020) 105932.
- [20] M.A. Postow, M.K. Callahan, J.D. Wolchok, Immune checkpoint blockade in cancer therapy, *J. Clin. Oncol.* 33 (2015) 1974–1982.
- [21] F. Xu, J.X. Chen, X.B. Yang, X.B. Hong, Z.X. Li, L. Lin, Y.S. Chen, Analysis of lung adenocarcinoma subtypes based on immune signatures identifies clinical implications for cancer therapy, *Mol. Ther. - Oncolytics* 17 (2020) 241–249.
- [22] F. Xu, X. Zhan, X. Zheng, H. Xu, Y. Li, X. Huang, L. Lin, Y. Chen, A signature of immune-related gene pairs predicts oncologic outcomes and response to immunotherapy in lung adenocarcinoma, *Genomics* 112 (2020) 4675–4683.
- [23] R. Bonneville, M.A. Krook, E.A. Kautto, J. Miya, M.R. Wing, H.Z. Chen, J.W. Reeser, L. Yu, S. Roychowdhury, Landscape of microsatellite instability across 39 cancer types, *JCO Precis. Oncol.* (2017) (2017).
- [24] K. Lee, J.W. Chang, C. Oh, L. Liu, S.N. Jung, H.R. Won, Y.I. Kim, K.S. Rha, B.S. Koo, HOXB5 acts as an oncogenic driver in head and neck squamous cell carcinoma via EGFR/Akt/Wnt/β-catenin signaling axis, *European journal of surgical oncology, The J. Eu. Soc. Surg. Oncol. the Br Ass. Surg. Oncol.* (2019).
- [25] G.A. McArthur, P.B. Chapman, C. Robert, J. Larkin, J.B. Haanen, R. Dummer, A. Ribas, D. Hogg, O. Hamid, P.A. Ascierto, C. Garbe, A. Testori, M. Maio, P. Lorigan, C. Lebbe, T. Jouary, D. Schadendorf, S.J. O'Day, J.M. Kirkwood, A.M. Eggermont, B. Dreno, J.A. Sosman, K.T. Flaherty, M. Yin, I. Caro, S. Cheng, K. Trunzer, A. Hauschild, Safety and efficacy of vemurafenib in BRAF(V600E) and BRAF(V600K) mutation-positive melanoma (BRIM-3): extended follow-up of a phase 3, randomised, open-label study, *The Lancet. Oncol* 15 (2014) 323–332.
- [26] T.C. Westbrook, I.S. Hagemann, J. Ley, K. Chen, K. Palka, J. Liu, L. Chen, P. Oppelt, D. Adkins, Prospective assessment of the clinical benefit of a tailored cancer gene set built on a next-generation sequencing platform in patients with recurrent or metastatic head and neck cancer, *37* (2019) 12.
- [27] C.C. Sun, S.J. Li, W. Hu, J. Zhang, Q. Zhou, C. Liu, L.L. Li, Y.Y. Songyang, F. Zhang, Z.L. Chen, G. Li, Z.Y. Bi, Y.Y. Bi, F.Y. Gong, T. Bo, Z.P. Yuan, W.D. Hu, B.T. Zhan, Q. Zhang, Q.Q. He, D.J. Li, Comprehensive analysis of the expression and prognosis for E2Fs in human breast cancer, *Mol. Ther.* 27 (2019) 1153–1165.
- [28] P.L. Peng, X.Y. Zhou, G.D. Yi, P.F. Chen, F. Wang, W.G. Dong, Identification of a novel gene pairs signature in the prognosis of gastric cancer, *7* (2018) 344–350.
- [29] F. Pagès, M. Berger A Fau - Camus, F. Camus M Fau - Sanchez-Cabo, A. Sanchez-Cabo F Fau - Costes, R. Costes A Fau - Molidor, B. Molidor R Fau - Mlecnik, A. Mlecnik B Fau - Kirilovsky, M. Kirilovsky A Fau - Nilsson, D. Nilsson M Fau - Damotte, T. Damotte D Fau - Meatchi, P. Meatchi T Fau - Bruneval, P.-H. Bruneval P Fau - Cugnenc, Z. Cugnenc Ph Fau - Trajanoski, W.-H. Trajanoski Z Fau - Fridman, J. Fridman Wh Fau - Galon, J. Galon, Effector memory T cells, Early Meta Surv. Colorectal Cancer.
- [30] E. Katsuta, Q. Qi, X. Peng, S.N. Hochwald, L. Yan, K. Takabe, Pancreatic adenocarcinomas with mature blood vessels have better overall survival, *9* (2019) 1310.
- [31] S. Edin, M.L. Wikberg, A.M. Dahlén, J. Rutegård, Å. Öberg, P.A. Oldenborg, R. Palmqvist, The distribution of macrophages with a M1 or M2 phenotype in relation to prognosis and the molecular characteristics of colorectal cancer, *PLoS One* 7 (2012) e47045.
- [32] R. Noy, J.W. Pollard, Tumor-associated macrophages: from mechanisms to therapy, *Immunity* 41 (2014) 49–61.
- [33] E. Sato, S.H. Olson, J. Ahn, B. Bundy, H. Nishikawa, F. Qian, A.A. Jungbluth, D. Frosina, S. Gnjatic, C. Ambrosone, J. Kepner, T. Odunsi, G. Ritter, S. Lele, Y.T. Chen, H. Ohtani, L.J. Old, K. Odunsi, Intraepithelial CD8+ tumor-infiltrating lymphocytes and a high CD8+/regulatory T cell ratio are associated with favorable prognosis in ovarian cancer, *Proc. Natl. Acad. Sci. U S A* 102 (2005) 18538–18543.

- [34] Y. Kurebayashi, H. Ojima, H. Tsujikawa, N. Kubota, J. Maehara, Y. Abe, M. Kitago, M. Shinoda, Y. Kitagawa, M. Sakamoto, Landscape of immune microenvironment in hepatocellular carcinoma and its additional impact on histological and molecular classification, *Hepatology* 68 (2018) 1025–1041.
- [35] D. Zeng, M. Li, R. Zhou, J. Zhang, H. Sun, M. Shi, J. Bin, Y. Liao, J. Rao, W. Liao, Tumor Microenvironment characterization in gastric cancer identifies prognostic and immunotherapeutically relevant gene signatures, *Cancer Immunol. Res.* 7 (2019) 737–750.
- [36] G.M. Konjević, A.M. Vuletić, K.M. Mirjačić Martinović, A.K. Larsen, V.B. Jurišić, The role of cytokines in the regulation of NK cells in the tumor environment, *Cytokine* 117 (2019) 30–40.
- [37] P. Zheng, Z. Zhou, Human Cancer Immunotherapy with PD-1/PD-L1 Blockade, *Biomark. Cancer* 7 (2015) 15–18.
- [38] S. Lyford-Pike, S. Peng, G.D. Young, J.M. Taube, W.H. Westra, B. Akpene, T.C. Bruno, J.D. Richmon, H. Wang, J.A. Bishop, L. Chen, C.G. Drake, S.L. Topalian, D.M. Pardoll, S.I. Pai, Evidence for a role of the PD-1:PD-L1 pathway in immune resistance of HPV-associated head and neck squamous cell carcinoma, *Cancer Res* 73 (2013) 1733–1741.
- [39] Y. Yang, Cancer immunotherapy: harnessing the immune system to battle cancer, *J. Clin. Invest.* 125 (2015) 3335–3337.
- [40] T. Shukuya, D.P. Carbone, Predictive markers for the efficacy of anti-PD-1/PD-L1 antibodies in lung cancer, *J. Thoracic. Oncol.* 11 (2016) 976–988.
- [41] L. Chen, X. Han, Anti-PD-1/PD-L1 therapy of human cancer: past, present, and future, *J. Clin. Invest.* 125 (2015) 3384–3391.
- [42] C. Luchini, F. Bibéau, M.J.L. Ligtenberg, N. Singh, A. Nottegar, T. Bosse, R. Miller, N. Riaz, J.Y. Douillard, F. Andre, A. Scarpa, ESMO recommendations on microsatellite instability testing for immunotherapy in cancer, and its relationship with PD-1/PD-L1 expression and tumour mutational burden: a systematic review-based approach, *Ann. Oncol.* 30 (2019) 1232–1243.
- [43] R.J. Hause, C.C. Pritchard, J. Shendure, S.J. Salipante, Classification and characterization of microsatellite instability across 18 cancer types, *Nat. Med.* 22 (2016) 1342–1350.